Experimental Studies of Shock Diffraction

Experimental Studies of Shock Diffraction

M K Quinn[1], N Gongora-Orozco[1], H Zare-Behtash[1], R Mariani[1], and K Kontis[1]

1 Introduction

Diffraction of a normal shock wave has been the subject of numerous studies, dating back work of Whitham [1]. A large number of the complex flow features present were highlighted in the well known work by Skews [2]. Fig. 1 shows the flow features behind a strong shock diffracting around a sharp corner. Skews showed that for angles greater than 75^o the flow features become independent of the corner angle making the flow is solely dependent on incident shock Mach number, M_1. For incident shock Mach numbers greater than $M_i = 2$, the flow features resemble those seen in Fig. 1; however, for Mach numbers $M_i < 2.0$ the flow does not expand to supersonic speeds according to the theory given by Sun and Takayama [3] meaning that there is no secondary shock (**Ss**) as the flow in region 2 can decelerate without shock waves. As the incident shock (**I**) diffracts around the corner, a slipstream (**SL**) is formed because the flow cannot follow the contour of the wall and therefore separates. The slipstream rolls up into a vortex (**V**) which begins to slowly propagate downstream.

Application of Schlieren imaging to this type of flow is relatively common and reasonably straightforward. However, the application of PIV to this type of problem, which incorporates both compressible and unsteady flow, has only been tried on a handful of occasions [4][5][6] mainly involving vortex propagation. This study will aim to capture the moving shock and the phenomena associated with its diffraction.

2 Experimental Setup

This study was carried out in the University of Manchester Aero-Physics Laboratory using the 25.4 x 25.4 mm mechanical-rupture, square shock tube. The driver

University of Manchester, George Begg Building, Sackville Street, Manchester, UK

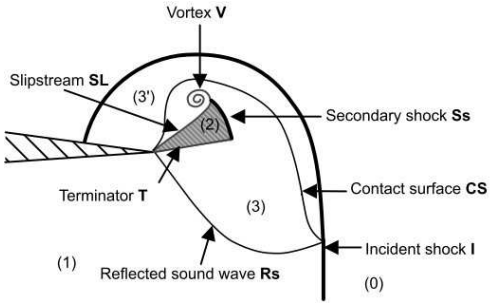

Fig. 1 Strong shock diffraction adapted from Skews [2]

and driven sections are 700 mm and 1700 mm respectively. The test section is 55.2mm high and made of 10 mm optical grade Perspex. The geometry tested has a knife edge tip and a wedge angle of $\theta = 6^o$. Driver section pressure measurements and camera triggering were performed using two Kulite XT-190M transducers connected to a NI USB-6251 16 bit M series Multifunction DAQ. The driver section of the shock tube was pressurised to $P_4 = 4$ bar while the driven was left at ambient giving a pressure ratio $P_4/P_1 = 4$.

2.1 High-Speed Schlieren Photography

The Schlieren setup used was a standard Z-style Toepler arrangement with a vertical knife edge. Continuous illumination came from an in-house constructed Xenon arc lamp. The flow was imaged using the Shimadzu HPV-1 which recorded 101 images at 250Kfps with an exposure time of 1μs. Images from the HPV-1 were stored on a Windows XP PC and were processed using ImageJ. The setup is almost identical to that used by Gongora-Orozco et al. [4].

2.2 Particle Image Velocimetry

Particle Image Velocimetry is a non-intrusive optical technique which measures the velocity of tracer particles carried by the fluid [7]. The PIV measurements were gathered using the TSI High-Speed, High Resolution Particle Image Velocimetry System incorporating the New Wave Research high power, high repletion rate Pegasus laser (10mJ at 1KHz). This is a dual cavity laser, meaning that the time between laser pulses can be as low as 1ns. The Photron APX-RS camera used has a full resolution of 1024 x 1024 pixels at up to 1500Hz. The inter-frame time between images is 2.5μs which is the limiting factor of this system. The implications of this will be

discussed later. A TSI 9307-6 oil droplet generator was used to seed both the driven and driver section with an average olive oil droplet size of approximately 1.5μm.

It should be noted that the Schlieren and PIV images were gathered on separate runs, firstly because the tracer particles would obscure the density gradients present in compressible flow, and secondly because the far wall of the test section was required to be painted black due to excess reflections captured by the PIV system.

3 Results

The theoretical shock strengths and Mach number is shown in table 1. Theoretical calculations were made using simple one-dimensional shock tube theory. The difference between experimental and theoretical Mach numbers is in part due to the accuracy of estimating the shock speed from the Schlieren images, but also due to the distance attenuation and formation decrement effects in shock tube flows [8].

Table 1 Shock wave properties

Diaphragm Pressure Ratio	Theoretical Shock Strength	Theoretical Shock Mach Number	Experimental Shock Mach Number (*estimated*)	Theoretical Induced Velocity	Experimental Induced Velocity
P_4/P_1	P_2/P_1	M_{it}	M_i	$U_t\ m/s$	$U\ m/s$
4	1.95	1.34	1.24	170	140

Fig. 2 shows 4 Schlieren images with the velocity vectors calculated from PIV superimposed. The PIV images were analysed using the Insight 3G software using a minimum window size of 24 x 24 pixels.

The diffracton profile is similar to those seen by other researchers [9][10][11].The Schlieren image clearly shows the shape of the shock wave as it traverses the test section. Fig. 3[a] shows the flow 20μs after the shock wave has reached the corner. The Schlieren and PIV images are in good agreement, showing the shape of the shock to be largely normal but becoming curved at the contact surface (**CS**) with an almost uniform velocity profile behind it. Other flow features such as the vortex shed from the corner are too small to see at this time.

Fig. 3[b] shows the flow after 40μs. By this time the incident shock still has a straight section; however, a larger portion of it is becoming curved as the corner signal begins to influence the shock front. The streamlines begin to diverge and follow the path of the slipstream allowing the flow to expand and therefore increase in velocity. This increase in velocity is more pronounced in Figs. 3[c] and 3[d] as it reaches just over 200 m/s. By 72μs the induced vortex is clearly visible in the Schlieren images. Due to the finite grid size used in the PIV measurements it is impossible to measure the internal structure of the vortex. The PIV results show

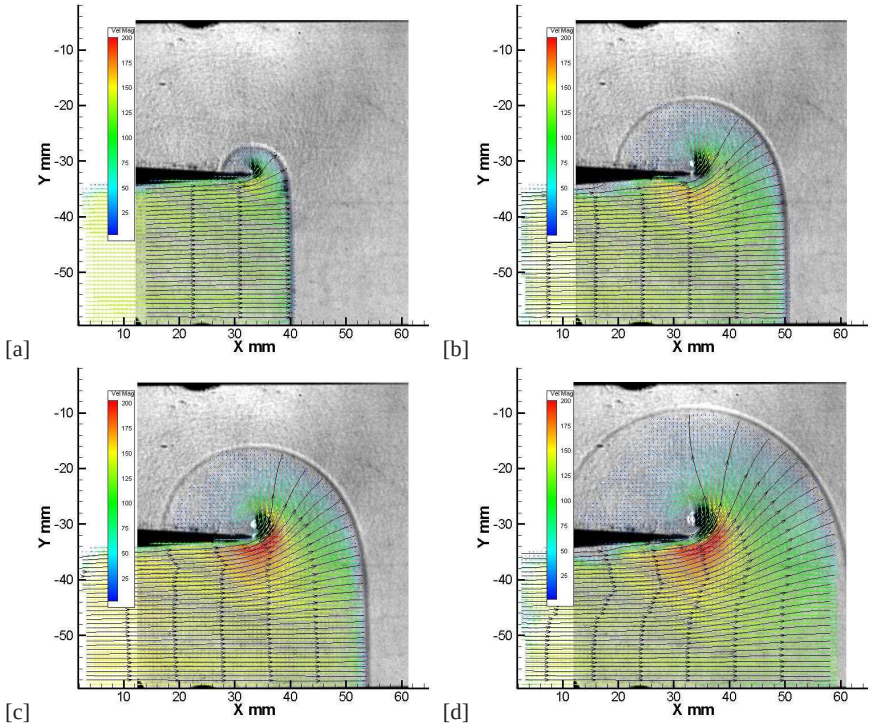

Fig. 2 Combined results with delay time [a] 20 μs [b] 40 μs [c] 48 μs [d] 7 2 μs

that flow in region 3 does not accelerate to the sonic speeds predicted by Sun and Takayama [3]. In this expansion region the image processing software often had trouble finding good correlation peaks. This is likely to be due to the blur effects described by Elsinga et al. [12].

Once the shock wave has diffracted around the corner, it is much weaker than before. This is to be expected; however, the level of attenuation is severe. The induced velocity behind the diffracted shock is significantly lower than the initial shock. This velocity was measured using a finer grid (16x16) than those shown in Fig. 3 as the maximum velocity is much smaller. It is intuitive to think that behind the diffracted shock the induced velocity will be lower; however, to the author's knowledge, this has not been quantified or demonstrated as clearly as this before.

3.1 Limitations

The applicability of a PIV system to high-speed, small-scale unsteady flow is dependant on minimum interrogation window size, camera resolution, minimum ΔT and particle characteristics. A minimum grid size of 24 x 24 pixels with a max-

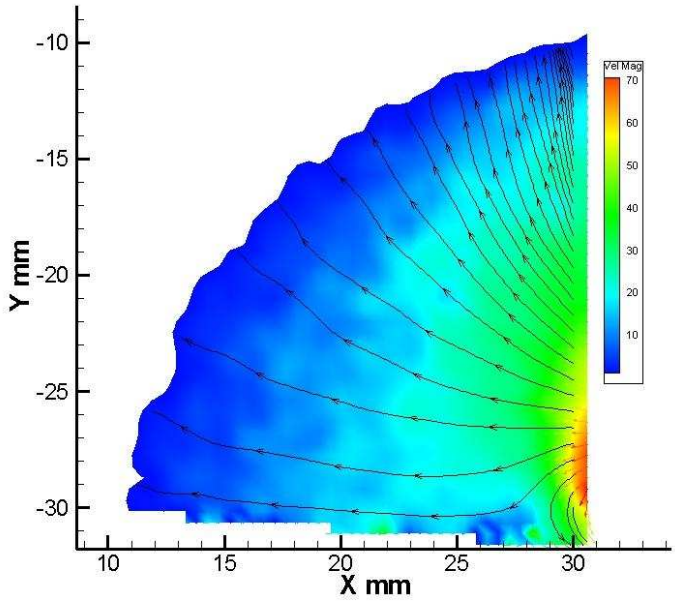

Fig. 3 Diffracted shock region at t = 72 μs

imum displacement ratio per window of 0.49 gives a maximum displacement of 11.76 pixles per ΔT. The scale of these images is 16.65 pixels per mm giving a maximum allowable travel of 0.706 mm per ΔT. With a minimum reliable ΔT of 2.5μs, the maximum velocity that can be measured using this system and a 24 x 24 window size is 282.52 m/s. If this window size is reduced to 16 x 16 pixels then the maximum velocity that can be measured reliably falls to 188.34 m/s, lower than the maximum velocity seen here.

Tracer particles in PIV do not exactly follow the flow, no matter how small and neutrally buoyant they are. This particle lag causes shock waves (a theoretically instantaneous velocity change) to be spread over a larger length scale, even upstream in some cases [13]. An estimation of the particle relaxation time τ is given by Melling [14] based on Stokes' drag law

$$\tau_s = \frac{{d_p}^2 \rho_p}{18\mu} \tag{1}$$

where d_p is the particle diameter, ρ_p its density and μ is the fluid viscosity. The average olive oil tracer particle size is approximately 1.5 μm, giving a relaxation time of 6.12 μs, giving a 90% rise time of 14.10 μs. Using the theory presented by Raffel et al. [7], integrating over the rise time gives a distance of 1.46 mm to reach 90% velocity. However, in truly unsteady flows, as we have here, the shock front has moved during this 14.10 μs rise time by 6.48 mm, giving a shock spread

of 5.02 mm. This is close to the data gathered from the PIV results where the 90% rise distance was measured as 4.56 mm.

4 Conclusion

This study aimed to capture small scale high-speed unsteady flow phenomena using PIV. The shape of a diffracting weak shock wave has been imaged using high-speed Schlieren photography along with velocity profiles gathered from high-speed PIV experiments. The results show that the incident shock wave induces an average velocity of 140 m/s, while the diffracted shock wave induces significantly less. The shock wave also induces a strong vortex emanating from the apex of the wedge. This vortex is not well resolved in the current experiments due to its small size.

This initial study into shock diffraction using PIV has proved that despite the large challenges of such an unsteady flow, reasonable results can be achieved. Future experiments are planned utilizing a higher resolution camera with a significantly lower inter frame time and finer seed particles resulting in greater accuracy.

5 Acknowledgements

The authors would like to thank the technical and administrative staff in the School of MACE at the University of Manchester. Special thanks go to the EPSRC (Engineering and Physical Sciences Research Council) Engineering Instrument Pool for loan of the Shimadzu HPV-1 and the TSI high-speed high resolution PIV system.

References

1. Whitham, G. B. - A new approach to problems of shock dynamics Part 1 Two-dimensional problems - Journal of Fluid Mechanics **2** (1957)
2. Skews, B. W. - The Perturbed Region Behind a Diffracting Shock Wave - Journal of Fluid Mechanics **29** (1967)
3. Sun, M. & Takayama, K. - A note on numerical simulation of vertical structures in shock diffraction - Shock Waves **13** (2003)
4. Gongora-Orozco, N., Zahre-Behtash, H., Kontis, K., Hale, C. - Particle image velocimetry studies on shock wave diffraction with co-flow jet - ISFV14 Korea (2010)
5. Zare-Behtash, H., Kontis, K., Gongora-Orozco, N., Takayama, K. - Shock wave-induced vortex loops emanating from nozzles with singular corners - Experiments in fluids **10** (2010)
6. Mariani, R. & Kontis, K. - Experimental studies on coaxial vortex loops - Physics of Fluids **22** (2010)
7. Raffel, M., Willers, C. E., Wereley, S. T., Kompenhans, J. - Particle image velocimetry: A practical guide - Springer Berlin (2007)
8. Emrich, J. R. & Wheeler, D. B. - Wall effects in shock tube flow - Physics of Fluids **1** (1958)

9. Hillier, R. - Computation of shock wave diffraction at a ninety degrees convex edge - Shock Waves **1** (1991)
10. Abate, G. & Shyy, W. - Dynamic structure of confined shocks undergoing sudden expansion - Progression in Aerospace Sciences **38** (2002)
11. Jiang, Z., Takayama, K., Babinsky, H., Meguro, T. - Transient shock wave flows in tubes with a sudden change in cross section - Shock Waves **7** (1997)
12. Elsinga, G. E., van Oudheusden, B. W., Scarano, F. - Evaluation of aero-optical distortion effects in PIV - Experiments in Fluids **39** (2005)
13. Havermann, M., Haertig, J., Rey, C., George, A.: PIV Measurements in shock tunnels and shock tubes In: *Particle Image Velocimetry*, ed by Schroeder, A. & Willert, C. E. (Springer Berlin / Heidelberg, 2008) pp 429-443
14. Melling, A. - Tracer particles and seeding for particle image velocimetry - Measurement Science Technology **8** (1997)